Enhanced Intracellular Protein Transduction by Sequence Defined Tetra-Oleoyl Oligoaminoamides Targeted for Cancer Therapy

*Peng Zhang, Dongsheng He, Philipp Michael Klein, Xiaowen Liu, Ruth Röder, Markus Döblinger, and Ernst Wagner**

Intracellular protein delivery presents a novel promising prospect for cell biology research and cancer therapy. However, inefficient cellular uptake and lysosomal sequestration hinder productive protein delivery into the cytosol. Here, a library of 16 preselected sequence-defined oligoaminoamide oligomers is evaluated for intracellular protein delivery. All oligomers, containing polyethylene glycol (PEG) for shielding and optionally folic acid as targeting ligand, manifest cellular internalization of disulfide-conjugated enhanced green fluorescent protein (EGFP). However, only a PEGylated folate-receptor targeted two-arm oligomer (729) containing both arms terminally modified with two oleic acids shows persistent intracellular protein survival and nuclear import of nlsEGFP (which contains a nuclear localization sequence) in folate-receptor-positive KB carcinoma cells, validating both effective endolysosomal escape and following subcellular transport. Furthermore, using ribonuclease A as a therapeutic cargo protein, among the tested oligomers, the oleic acid modified targeted two-arm oligomers exert the most significant tumor cell killing of KB tumor cells. An investigation of structure–activity relationship elucidates that the incorporated oleic acids play a vital role in the enhanced intracellular protein delivery, by promoting stable formation of 25–35 nm lipo-oligomer protein nanoparticles and by membrane-active characteristics facilitating intracellular cytosolic delivery.

1. Introduction

Protein therapeutics[1] have gained increasing attention due to their great potential in the treatment of many diseases. For cancer, they may provide a higher functional specificity and less genetic risks than standard nontargeted chemotherapies. Intracellularly active proteins present a therapeutic subclass which due to delivery problems still is in its early stage. Nevertheless, immunotoxins[2] have been evaluated in cancer patients.[3] Also Onconase,[4] a member of the ribonuclease A (RNase A) family,[3,5] which after uptake by cancer cells can degrade the cytosolic RNA and elicit tumor cell killing, has been clinically tested. In general, poor cellular uptake and especially endolysosomal entrapment hamper effective protein transduction into the cytosol. Cargo proteins are largely sequestrated and degraded in the endolysosomes without access to the subcellular target sites for subsequent biological actions. Therefore, novel delivery technologies are required to cope with the encouraging future opportunities of intracellular protein transfer ("protein transduction").[6] Amongst other technologies, biodegradable microgel encapsulation,[7] nanocapsules,[8] polymer micelles,[9] lipid-like nanoparticles,[10] virus-like protein nanoparticles,[11] or coupling with peptide transduction domains[12] have been pursued. Here we present bioreversible conjugation of the cargo protein with precise sequence-defined oligoaminoamide carriers as an alternative encouraging option.

Using solid-phase synthesis technology, we recently synthesized such cationic oligomers based on artificial amino acid blocks (e.g., succinoyl tetraethylene pentamine, Stp; succinoyl pentaethylene hexamine, Sph) which were assembled into precise sequences, and demonstrated their efficient capacity in delivery of pDNA and siRNA polyplexes.[13] Furthermore, receptor ligand and polyethylene glycol (PEG) modified oligomers were successfully generated for targeted nucleic acid delivery.[14] This work revealed the endolysosomal barrier as a critical hurdle, and resulted in the design of endosomolytic domains such as fatty acids[13a,15] or endosomally protonatable units.[14a] These units, when incorporated into oligomers, dramatically increased nucleic acid transfection. We hypothesized that the novel precise carriers might be useful also as delivery domains in conjugates of proteins or other drugs.[16] In initial work, one sequence-defined three-arm cationic oligomer had been conjugated with proteins by bioreducible disulfide[17]

P. Zhang, D. He, P. M. Klein, X. Liu, R. Röder, Prof. E. Wagner
Pharmaceutical Biotechnology
Center for System-based Drug Research
Ludwig-Maximilians-University
Munich 81377, Germany
E-mail: ernst.wagner@cup.uni-muenchen.de

P. Zhang, D. He, P. M. Klein, X. Liu, R. Röder, Prof. E. Wagner
Center for NanoScience (CeNS)
Ludwig-Maximilians-University
Munich 81377, Germany

Dr. M. Döblinger
Department of Chemistry
Ludwig-Maximilians-University
Munich 81377, Germany

DOI: 10.1002/adfm.201503152

linkage for delivery of nlsEGFP or β-galactosidase into cells. In the current work, 16 PEGylated two-arm and four-arm oligomers optionally containing folic acid for cell receptor targeting were selected and evaluated for targeted intracellular protein transduction. Different artificial amino acid building blocks, as well as protonatable histidines, or oleic acids were included to enhance endosomolytic ability. All these oligomers were coupled to nlsEGFP or RNase A by disulfide bonds, respectively. The disulfide linkages are supposed to be cleaved in the reducing cytosolic environment after endolysosomal escape.[18] Our new results show that the oleic acid modified targeted sequence-defined oligomers very potently transduce nlsEGFP and RNase A into the cytosol, where nlsEGFP undergoes efficient delivery into the nucleus, and RNase A triggers most effective killing of folate-receptor-positive cancer cells.

2. Results and Discussion

2.1. Synthesis of Oligoaminoamide–Protein Conjugates

From an existing library of more than 900 precise cationic oligoaminoamides, 16 candidates were chosen for in-depth evaluation of intracellular protein delivery. All oligomers were manufactured by solid-phase supported synthesis to gain precise chemical structures in defined sequences and topologies. Folic acid was conjugated to the cationic backbone for receptor mediated protein transduction through a monodisperse PEG (PEG24) chain, which can help to reduce the unspecific interactions between nanocarriers and the biological environment. The backbones of different oligomers have different topologies, such as two-arm, three-arm, and four-arm,[13a] and consist of novel artificial amino acid building blocks (e.g., Stp, Sph) as basic functional units for endosomal escape.[14a] Oleic acids were incorporated into oligomers to enhance endosomal escape and nanoparticle stabilization.[13a,15] Moreover, natural amino acids were included in these oligomers: lysines were included as branching points (by selective modification both at α- and ε-amino groups), histidines[14a] to promote proton sponge effect enhancing endolysosomal escape, tyrosines[19] and cysteines[18d,e] were coupled to facilitate association of conjugates by aromatic ring interactions or reducible disulfide bonds, respectively. Cysteines also act as bioreducible attachment sites for the cargo proteins. Different substitutes for folic acid (glutamic acid, glutaric acid, alanine) were used in the nontargeted control oligomers. Sequences and topology are shown in **Table 1**.

Two representative proteins, nlsEGFP and RNase A, were employed to evaluate targeted intracellular protein delivery. Recombinant nlsEGFP[20] contains a nuclear localization sequence (NLS) derived from SV40 large T-antigen. This sequence can help nlsEGFP in migrating from cytosol into the nucleus by natural mechanisms. Hence, based on this property, nlsEGFP can be utilized to characterize endolysosomal escape and subcellular nuclear transport by fluorescence microscopy. Meanwhile, RNase A[5a] when internalized into the cytosol of cancer cells can degrade the cellular RNA and induce cell killing.

The conjugation process of the various oligomers to the model proteins (nlsEGFP, RNase A) is shown in **Scheme 1**A.

Table 1. Oligoaminoamide oligomers for protein conjugation. Abbreviations: FolA: folic acid; GlutA: glutaric acid; OA: oleic acid; E: glutamic acid; C: cysteine; H: histidine; K: branching lysine selectively modified at α and ε amines; Y: tyrosine; A: alanine; PEG_{24}: polyethylene glycol containing 24 ethylene oxide monomer units.

Sequence (C to N terminal)	ID	Topology
K-ε (PEG_{24}-E)-K-α,ε (Sph_3-Y_3-C)$_2$	714	Two-arm
K-ε (PEG_{24}-FolA)-K-α,ε (Sph_3-Y_3-C)$_2$	715	
K-ε (PEG_{24}-E)-K-α,ε (Stp_4-C-K-OA_2)$_2$	728	
K-ε (PEG_{24}-FolA)-K-α,ε (Stp_4-C-K-OA_2)$_2$	729	
K-ε (PEG_{24}-GlutA)-K-α,ε (Stp_4-C)$_2$	937	
K-ε (PEG_{24}-FolA)-K-α,ε (Stp_4-C)$_2$	737	
K-ε (PEG_{24}-E)-K-α,ε [(H-Stp)$_4$-H-Y_3-C]$_2$	794	
K-ε (PEG_{24}-FolA)-K-α,ε [(H-Stp)$_4$-H-Y_3-C]$_2$	795	
C-(Stp)$_3$-K-α,ε [(Stp)$_3$-C]$_2$	386	Three-arm
K-ε (PEG_{24}-A)-K-α,ε [K-α,ε (Sph_3-C)$_2$]$_2$	706	Four-arm
K-ε (PEG_{24}-FolA)-K-α,ε [K-α,ε (Sph_3-C)$_2$]$_2$	707	
K-ε (PEG_{24}-E)-K-α,ε [H-K-α,ε (H-Sph)$_3$-H-C)$_2$]$_2$	712	
K-ε (PEG_{24}-FolA)-K-α,ε [H-K-α,ε (H-Sph)$_3$-H-C)$_2$]$_2$	713	
K-ε (PEG_{24}-E)-K-α,ε [K-α,ε (Stp_3-C)$_2$]$_2$	732	
K-ε (PEG_{24}-FolA)-K-α,ε [K-α,ε (Stp_3-C)$_2$]$_2$	733	
K-ε (PEG_{24}-E)-K-α,ε [H-K-α,ε ((H-Stp)$_3$-H-C)$_2$]$_2$	761	
K-ε (PEG_{24}-FolA)-K-α,ε [H-K-α,ε ((H-Stp)$_3$-H-C)$_2$]$_2$	762	

Biologically reducible N-succinimidyl 3-(2-pyridyldithio)propionate (SPDP) linkers were utilized to covalently attach oligomers to nlsEGFP or RNase A through disulfide bonds. On average, every nlsEGFP molecule was modified with three SPDP linkers, for RNase A, two SPDP linkers were introduced per protein molecule. Following endolysosomal escape, the formed disulfide linkages are supposed to be cleaved by cytosolic reducing glutathione (GSH). As a result, oligomer free nlsEGFP or RNase A will be obtained. As shown in Figure S1 (Supporting Information), nlsEGFP and RNase A were successfully modified with representative oligomers (728, 729, 937, 737). The treatment of nlsEGFP and RNase A conjugates with reducing GSH at cytosolic concentration (5×10^{-3} M) generated oligomer free nlsEGFP or RNase A. These results prove that the modification of proteins with oligomers by disulfide bonds is biologically reversible at physiological conditions. The other oligomers also exhibited successful modification of proteins and biological reversibility of disulfides linkages (data not shown). In aqueous solution, the protein conjugates spontaneously form nanoparticles, with the sizes and surface charges determined by dynamic light scattering (DLS, see Table S1, Supporting Information, for nlsEGFP; Table S2, Supporting Information, for RNase A) strongly depending on the selected oligomer. Consistent with the intrinsic properties of the cargo proteins, the conjugates of RNase A (smaller, more basic protein) formed slightly smaller (23–600 nm) and more positively charged (zeta potential up to +22 mV) nanoparticles as compared to the nlsEGFP conjugates (30 nm to >1 μm; zeta up to 14 mV). Notably, only the lipo-oligomers 728 and 729 (chemical structures shown in Scheme 1B) mediated the formation of

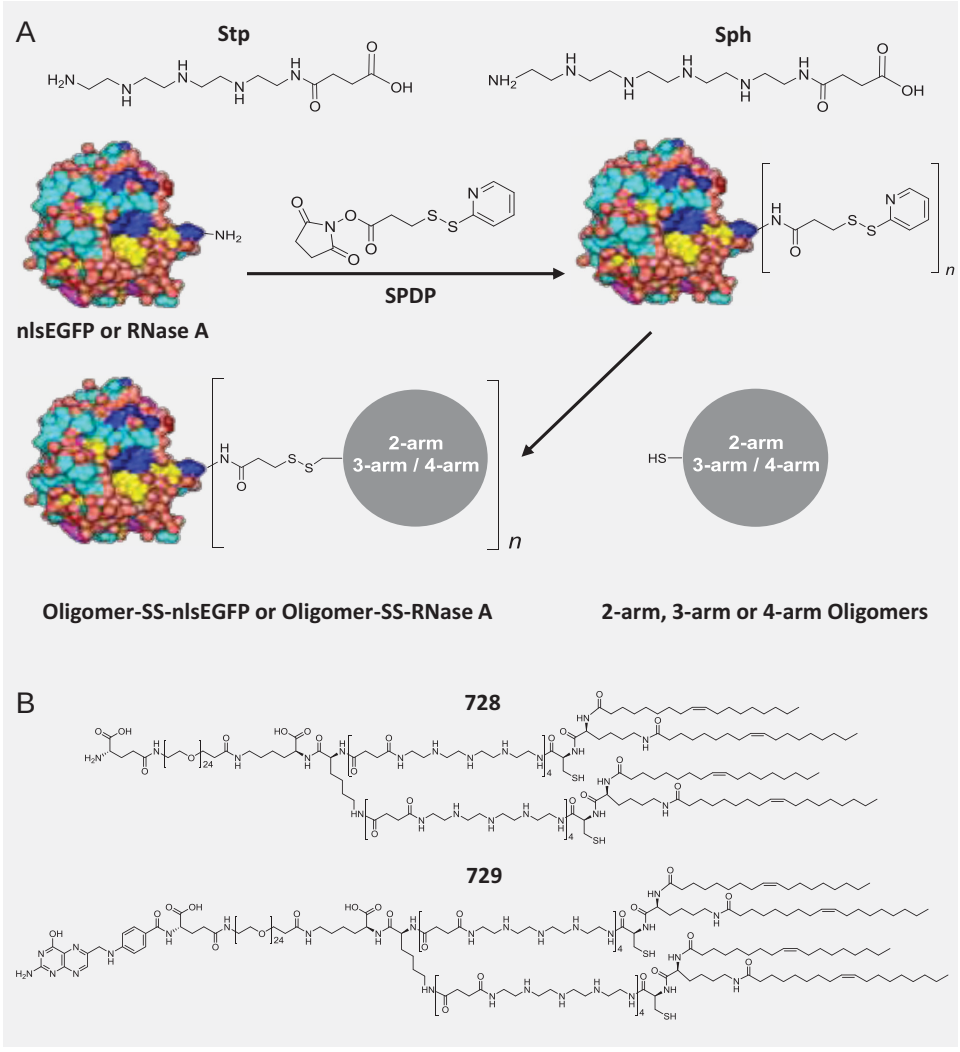

Scheme 1. A) Modification of nlsEGFP or RNase A with Stp or Sph containing two-, three-, or four-arm oligomers (Table 1) via bioreducible SPDP linkers. Number of oligomers (*n*) covalently coupled to the protein: $n = 3$ (in average) for nlsEGFP, $n = 2$ (in average) for RNase A. Conjugates spontaneously form nanoparticles. B) Chemical structures of oleic acid modified 2-arm oligomer 728 and 729.

small nanoparticles with average sizes of 23–25 nm and +20 mV zeta potential for RNase A conjugates, and 30–36 nm and +14 mV zeta for nlsEGFP conjugates. The transmission electron microscopy (TEM) image of representative 729-SS-RNase A conjugates (Figure S2, Supporting Information) showed a homogeneous distribution of the nanosized conjugates, with a uniform size of an average diameter of ≈10 nm and elliptical or worm-like shape (length >10 nm). The discrepancy between TEM and the larger (25 nm) size measured by DLS may be explained by the extended worm-like shape and because TEM was performed in vacuum state where conjugate size would shrink.

2.2. Screening of Oligomer–nlsEGFP Conjugates Reveals Oleoyl-Modified Oligomer 729 as Potent Transduction Carrier

To evaluate the protein delivery efficiency and folate receptor specificity of the targeted oligomers, cells were transfected with nlsEGFP conjugates in standard serum-containing medium as described in the Experimental Section. Flow cytometry was used to quantify the fluorescence intensity. Figure S3 (Supporting Information) demonstrates that all the conjugates showed nice cellular association and internalization already after a short 45 min incubation. The four-arm targeted oligomer conjugates (707, 713, 733, 762) did not display significantly better association and internalization compared with the conjugates of their nontargeted control oligomers. The two-arm targeted oligomer conjugates, 715 and 729, manifested far higher cell binding and uptake than their nontargeted controls. The lower specificity of the four-arm oligomer conjugates can be well explained by their higher numbers of positive charges and/or more disulfide crosslinks. The high positive charge can induce unspecific association on cells and more crosslinks may prevent folate acid arising on conjugates surface. Free folic acid competition experiment was also performed to further confirm the folate receptor specificity of 729-SS-nlsEGFP. The results (Figure S4, Supporting Information) revealed that free folic

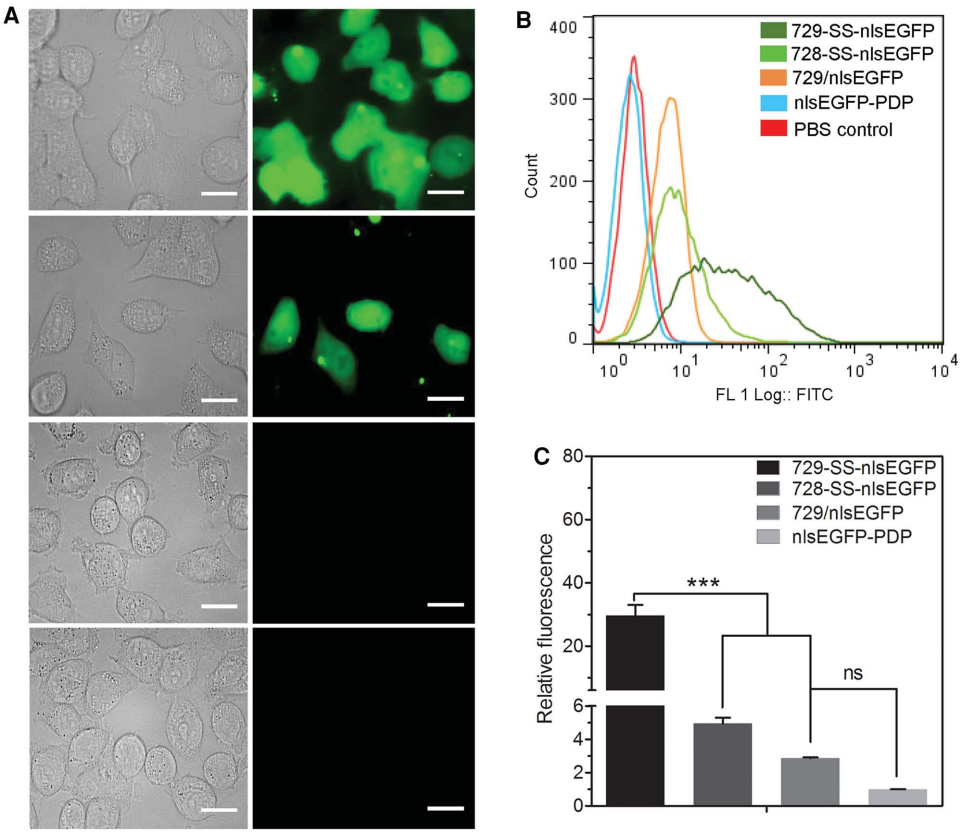

Figure 1. Transduction of KB cells with 729-SS-nlsEGFP (FolA-targeting) compared to 728-SS-nlsEGFP (nontargeted) mediated protein transduction. A) Fluorescence microscopy of the live KB cells treated with 1×10^{-6} M 729-SS-nlsEGFP (row 1), 1×10^{-6} M 728-SS-nlsEGFP (row 2), mixtures of 6×10^{-6} M 729 and 1×10^{-6} M free nlsEGFP (row 3), and 1×10^{-6} M nlsEGFP-PDP (row 4) for 24 h, followed by a 24 h incubation in fresh media. Left column: Bright-field images of the treated cells. Right column: EGFP fluorescence of the treated cells. B) Cellular internalization of each sample incubated with KB cells as described in (A). C) Relative fluorescence intensities of cells treated with each sample as described in A). The intensities were normalized regarding the mean fluorescence intensity of the cells treated with nlsEGFP-PDP. ***$p < 0.001$; ns: no significant difference. Data are shown as mean ± SD ($n = 3$). Scale bar = 20 μm.

acid competition significantly inhibited the cellular association and slightly inhibited the cellular internalization of 729-SS-nlsEGFP. Furthermore, the fluorescence intensity was investigated after incubating cells with the nlsEGFP conjugates for 24 h, followed by an additional 24 h incubation in fresh media (Figure S5, Supporting Information). The fluorescence intensity was supposed to be reduced because of cell proliferation and/or degradation of nlsEGFP by proteases in lysosomes if entrapped. Cells treated with 712, 713, 728, 729, 794, and 795 nlsEGFP conjugates however remained (22%–92%) enhanced green fluorescent protein (EGFP) fluorescence-positive, whereas the cells treated with the other conjugates (706, 707, 714, 715, 732, 733, 761, 762) had lost nlsEGFP fluorescence (<10%). Compared with 706 and 707, respectively, 712 and 713 nlsEGFP conjugates had a higher recovery of EGFP fluorescence. This can be attributed to the histidines in the oligomers which have been reported to increase the buffer capacity, enhancing endosomal escape or postponing the lysosomal acidification required for protease bioactivities. These effects of histidines may help nlsEGFP to escape from protease degradation. It is noteworthy that 729-SS-nlsEGFP showed the highest percentage of fluorescence-positive cells (92%) among all the conjugates. This initial screen indicated that 729 may be a potent nanocarrier for targeted protein delivery.

Fluorescence microscopy confirmed the capacity of these oligomers to deliver nlsEGFP into cells, promote endolysosomal escape, and subsequent subcellular trafficking into the nucleus. **Figure 1**A displays that 729-SS-nlsEGFP and 728-SS-nlsEGFP treated cells presented homogeneous fluorescence throughout the cells for 24 h after an incubation time of 24 h. However, cells treated with the other conjugates showed no fluorescence or just punctate fluorescence under the fluorescence microscope (data not shown). This suggests that 729-SS-nlsEGFP and 728-SS-nlsEGFP successfully escaped from endosomes/lysosomes and were reduced in the cytosol, resulting in oligomer-free nlsEGFP all over the cells. Moreover, nlsEGFP was found imported into the cell nuclei, compared with only cytosolic location (presented by dark appearance of the nuclei) as observed in previous work,[20] which also validates the successful endosomal escape of 729-SS-nlsEGFP and 728-SS-nlsEGFP, the biological reversibility of conjugation, and subsequent nuclear translocation mediated via the NLS signal. The nlsEGFP was not concentrated in the nucleus, which may result from incomplete release of nlsEGFP from the carrier or linker, as the

Table 2. Summary of the intracellular nlsEGFP delivery efficacy of various targeted nlsEGFP conjugates (indicated by oligomer ID number).

Conjugates (oligomer-SS-nlsEGFP)	Cellular association	Cellular internalization	Target specificity	EGFP positive cells [48 h, %]	Nuclear import
707	+[a)]	+	–[b)]	10	–
713	+	+	–	58	–
715	+	+	+	6	–
729	+	+	+	92	+
733	+	+	–	2	–
762	+	+	–	7	–
795	+	+	–	22	–

[a)]+: positive; [b)]–: negative.

NLS (Pro-Lys-Lys-Lys-Arg-Lys-Val) of nlsEGFP is rich in lysines, it is quite possible that some NLS lysines are irreversibly amidated by the SPDP linker. Such modified NLS would not work as a nuclear localization signal.

In contrast, SPDP modified nlsEGFP and the mixture of 729 and free nlsEGFP without covalent attachment had very low efficiency to enter the treated cells (not detectable by fluorescence microscopy). The performances of the targeted FolA-containing 729 conjugate and the nontargeted glutamate-containing 728 conjugate can be directly compared by microscopy and flow cytometry. More EGFP positive cells were observed in the fluorescence microscope images of 729-SS-nlsEGFP treated than 728-SS-nlsEGFP treated cells. This was confirmed by flow cytometry. Cells treated with SPDP modified nlsEGFP present almost the same fluorescence background intensity as phosphate buffered saline (PBS) treated cells (Figure 1B). Cells incubated with a mixture of 729 and free nlsEGFP display only slightly higher fluorescence. Importantly, 729-SS-nlsEGFP treated cells displayed a significantly higher mean fluorescence intensity, sixfold higher than that of cells treated with nontargeted 728-SS-nlsEGFP, and tenfold higher than that of cells treated with the mixture of 729 and free nlsEGFP (Figure 1C). These results suggest that FolA-targeted 729-SS-nlsEGFP shows more efficient and effective nlsEGFP transduction ability as compared to the nontargeted 728-SS-nlsEGFP. Covalent conjugation by disulfide bonds plays a decisive role in the nlsEGFP transfection. This was demonstrated by the ineffectiveness of the mixtures of 729 and free nlsEGFP. In conclusion, it is noteworthy that 729-SS-nlsEGFP is the only conjugate presenting nice cellular association, cellular internalization, folate receptor specificity, long-term (48 h) survival of nlsEGFP activity, and subcellular nuclear import among all the targeted oligomers (**Table 2**).

2.3. Folate-PEG-Oleoyl Containing Two-Arm Oligomer 729-SS-RNase A Conjugate Triggers Potent KB Carcinoma Cell Killing

To further compare their protein delivery efficiency, oligomers were conjugated with RNase A as therapeutic cargo protein at a molar ratio of 4:1. This oligomer/cargo protein ratio was empirically found as most effective. Successful delivery of RNase A into the cytosol was expected to elicit degradation of cytosolic RNA, thereby inducing cell killing. KB cells were treated with the various oligomers, the corresponding oligomer/RNase A noncovalent mixtures as controls, or the oligomer–RNase A conjugates, and the metabolic cell activity after 48 h was determined using an dimethylthiazolyl-diphenyltetrazolium bromide (MTT) assay (**Figure 2**A). Cells treated with oligomers only showed no or only low (up to 25%) reduction in metabolic activity. The corresponding dose of SPDP linker modified RNase A did also not result in any detectable change of cell viability, which can be attributed to the lack of

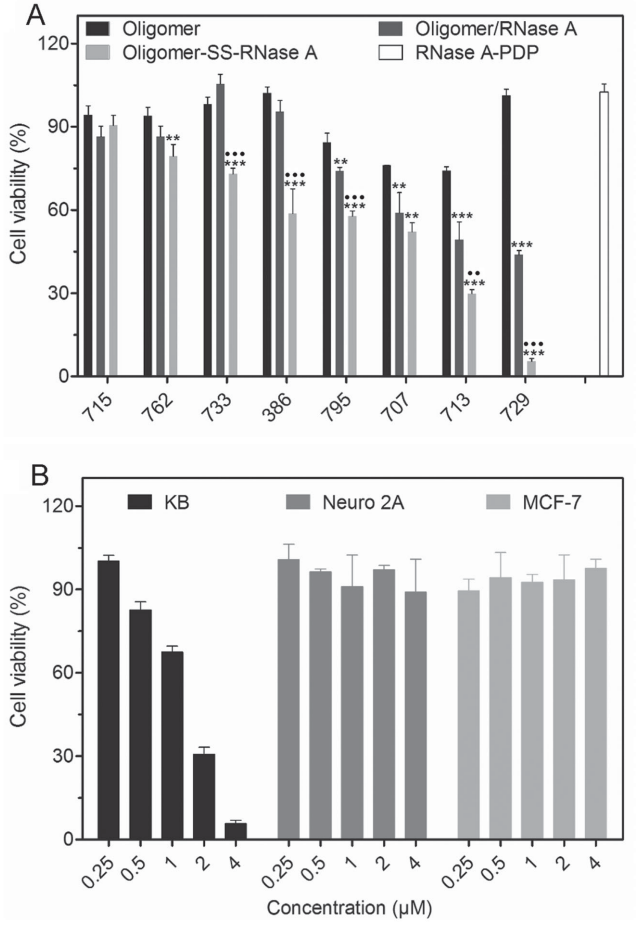

Figure 2. A) Evaluation of RNase A transfection efficiency with various RNase A conjugates on KB cells presented as % cell metabolic activity of control cells (MTT assay). Cells were incubated with the indicated agents under standard culture conditions for 4 h, followed by a 44 h incubation with fresh media. Black: oligomer control (16×10^{-6} M); deep gray: mixtures of oligomer (16×10^{-6} M) and free RNase A (4×10^{-6} M); gray: RNase A conjugates (4×10^{-6} M); white: RNase A-PDP (4×10^{-6} M). B) Protein concentration-dependent cytotoxicity of 729 mediated RNase A transfection on folate-receptor-positive KB cells in comparison to folate-receptor-negative cells (MCF-7 and Neuro 2A). *: compared with oligomer; •: compare with oligomer/RNase A. **$p < 0.01$, ***$p < 0.001$, •$p < 0.01$, ••$p < 0.001$. Data are shown as mean ± SD ($n = 3$).

intracellular delivery for SPDP modified RNase A. Unmodified RNase A was also nontoxic (data not shown).

In contrast, the RNase A conjugates formed with various oligomers exhibited cytotoxicity. Five targeted oligomers (707, 713, 729, 733, 795) and their nontargeted control oligomers (706, 712, 728, 732, 794 in Figure S6, Supporting Information) could successfully deliver RNase A into tumor cells and reduce their viability. The three-arm oligomer 386, previously reported as carrier for nlsEGFP delivery, could transduce RNase A into cells resulting in moderate (40%) reduction of cell viability. Cells treated with the mixtures of free RNase A and oligomers also presented appreciable reduction of metabolic activity. Such an effect of noncovalent mixtures was not observed in the nlsEGFP delivery (Figure 1A) and is presumably based on the special properties of RNase A. The intrinsic positive charge of RNase A (pI 9.6) enables the protein to bind to the negatively charged cell membrane; simultaneous internalization of membrane-bound RNase A with the endosomolytic oligomers, as a result, may indirectly mediate endosomal release into the cytosol, analogously as observed elsewhere.[21] The covalent conjugates, however, always displayed a far higher cytotoxicity than the mixtures. Consistent with the nlsEGFP transfection results, the RNase A conjugates of histidinylated oligomers 712 and 713 showed higher cytotoxicity than those of the histidine-lacking analogs 706 and 707, respectively. Among all the tested conjugates, 729-SS-RNase A (Figure 2A) and its nontargeted 728 analog (Figure S6, Supporting Information) mediated the by far highest cytotoxicity, decreasing the viability of KB cells down to 5%, whereas the toxicity of the free oligomer was negligible.

Based on the promising RNase A delivery efficiency, 729-SS-RNase A was evaluated in more detail. Figure 2B presents the protein dose dependence of cytotoxicity. Interestingly, no significant decrease in cell viability was observed in folate-receptor-negative cells (MCF-7 and Neuro-2a) after incubation with 729-SS-RNase A conjugate at the same concentrations. It remains to be determined whether the major reasons are (i) reduced cellular uptake due to lack of target receptor or (ii) reduced sensitivity toward internalized RNase A, for example by different levels of natural cytosolic ribonuclease inhibitor,[5a] the main physiological inhibitor of RNase A. In our previous siRNA delivery work, gene silencing was less challenging in Neuro-2a cells than in KB cells,[15,22] arguing against alternative (i) as exclusive reason. Preference of RNase in killing a series of tumor cells as opposed to normal cells has been reported in the literature, with reasons which go beyond delivery and are still not fully understood.[4,5]

The cellular internalization and intracellular distribution of 729-SS-RNase A in KB cells was also investigated using fluorescein isothiocyanate (FITC) labeled RNase A to obtain 729-SS-RNase A-FITC conjugates. Fluorescence microscopy (**Figure 3**A) showed that free RNase A-FITC-PDP could not

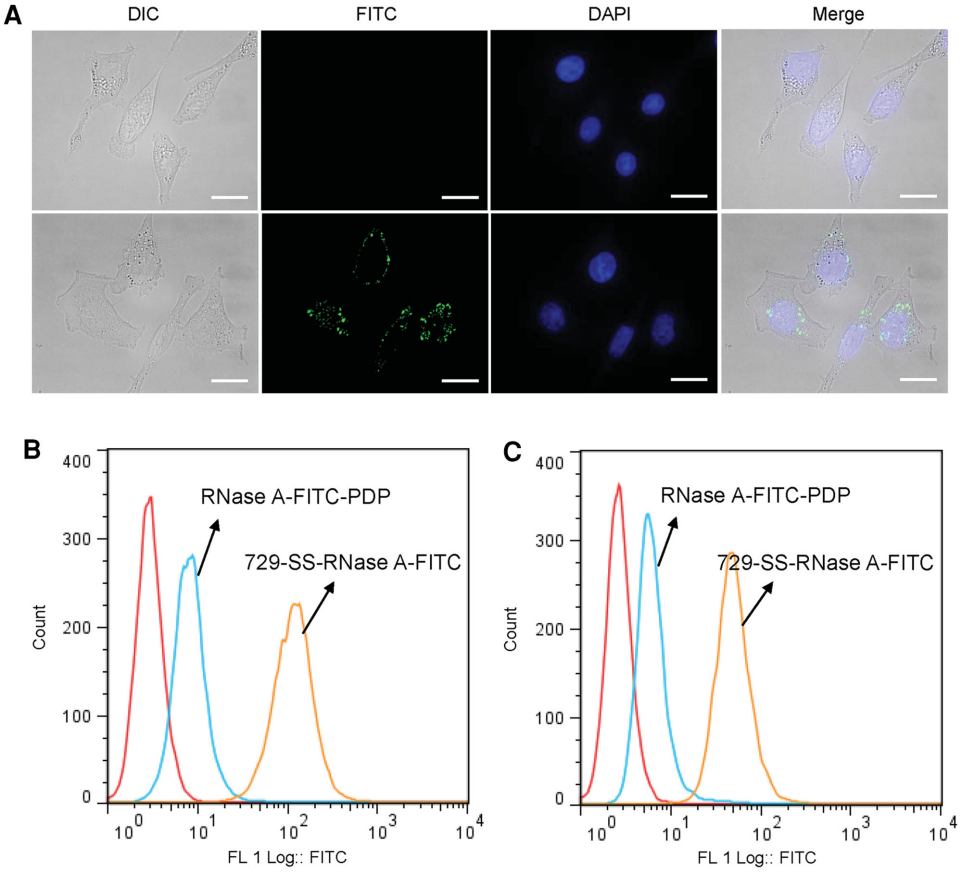

Figure 3. Transduction of KB cells with 729-SS-RNase A-FITC. A) Fluorescence microscopy of the KB cells treated with 2×10^{-6} M RNase A-FITC-PDP (row 1) or 2×10^{-6} M 729-SS-RNase A-FITC (row 2) for 45 min short incubation. B) Cellular association and C) cellular internalization after 45 min incubation with KB cells as determined by flow cytometry. Scale bar = 20 μm.

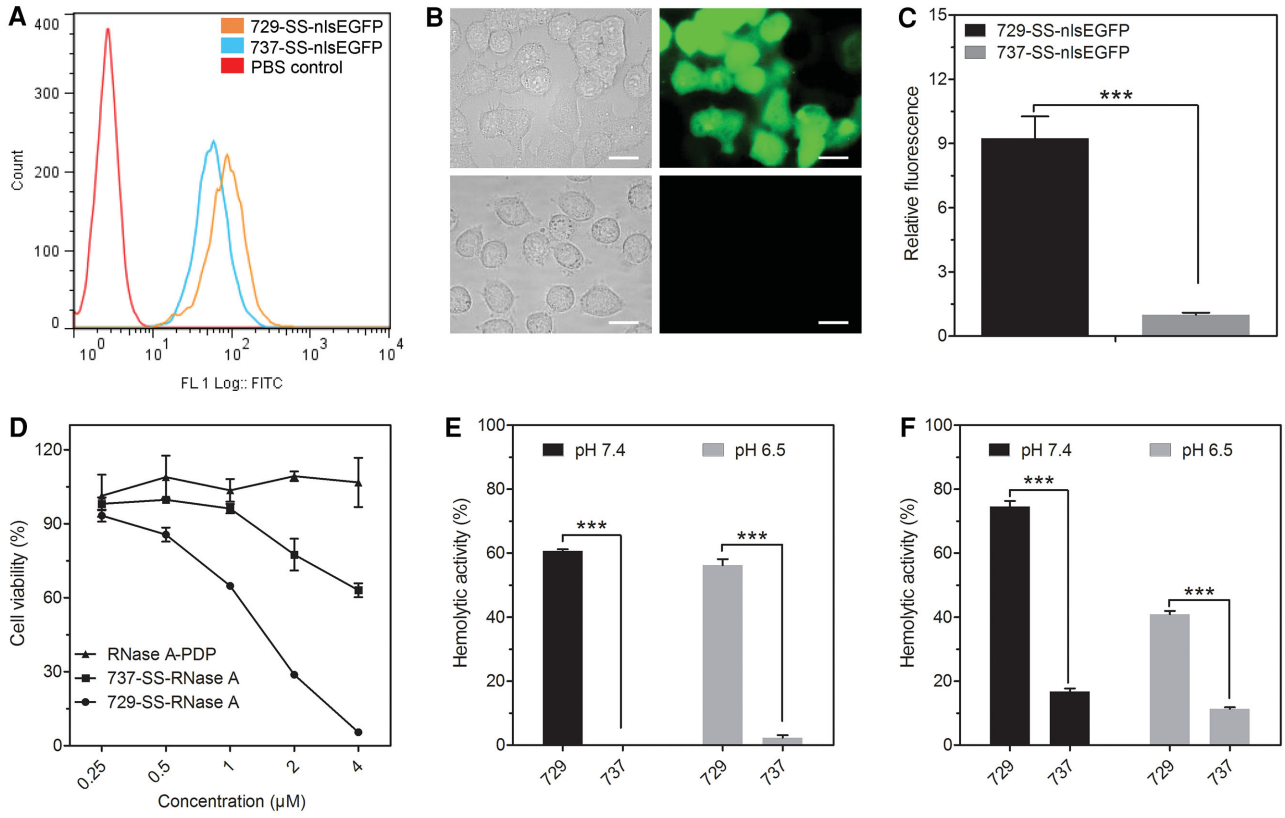

Figure 4. Structure–activity relationship of 729 enhanced intracellular protein delivery. A) Cellular internalization of 1×10^{-6} M 729 (oleic acid modified) or 737 (lacking oleic acids) targeted nlsEGFP conjugates after 45 min incubation with KB cells as determined by flow cytometry. B) Fluorescence microscopy of live KB cells treated with 1×10^{-6} M 729-SS-nlsEGFP (row 1) or 1×10^{-6} M 737-SS-nlsEGFP (row 2) for 24 h, followed by an incubation of 24 h in fresh media. Left column: Bright-field images of the treated cells. Right column: EGFP fluorescence of the treated cells. C) Relative fluorescence intensities per cell after in total 48 h after treatment as described in B). The intensities were normalized regarding the mean fluorescence intensity of cells treated with 737-SS-nlsEGFP. D) Evaluation of RNase A transduction with 729 or 737 RNase A conjugates on KB cells by using a cell metabolic activity (MTT) assay. E) Lytic activity of 729 or 737 nlsEGFP conjugates (1×10^{-6} M) at physiological pH 7.4 and early endosomal pH 6.5 in an erythrocyte leakage assay. F) Lytic activity of 729 or 737 RNase A conjugates (2×10^{-6} M) at pH 7.4 and pH 6.5. ***$p < 0.001$. Data are shown as mean ± SD ($n = 3$). Scale bar = 20 μm.

efficiently enter cells, as evidenced by lack of green fluorescence. In contrast, for 729-SS-RNase A-FITC treated cells, already after a relatively short 45 min incubation, a remarkable cellular uptake of 729-SS-RNase A-FITC and intracellular accumulation in endosomes was visible as green punctuate fluorescence. The different cell association and internalization efficiencies of 729-SS-RNase A-FITC and free RNase A-FITC-PDP were also confirmed and quantified by flow cytometry evaluation (Figure 3B,C), revealing again that 729 is a potent nanocarrier for protein delivery.

2.4. The Key Role of Oleic Acids in Oligomer 729—Facilitating Enhanced Cytosolic Entry via Lipid Membrane Destabilization and Subsequent Cell Killing by RNase A

The former results clearly demonstrate that 729 outperformed other oligomers with endosomal escape function, such as the four-arm oligomer comprising Sph and histidines, in protein delivery. We conclude that the oleic acids as the endosomolytic unit in 729 play a crucial role in the enhanced intracellular protein delivery. Therefore, based on this hypothesis, control oligomers (937, 737) with the same sequence, without or with folate targeting ligand, PEG and topology as in 728 or 729 except the oleic acids were synthesized, analyzed, and compared for protein delivery efficiency. After a 45 min incubation, folate-targeted 737-SS-nlsEGFP in comparison to the 729-SS-nlsEGFP conjugate displayed an only slightly reduced cell association (Figure S7, Supporting Information) and intracellular uptake (**Figure 4**A) as analyzed by flow cytometry. This suggests that the oleic acids do not have a significantly enhancing effect on cellular binding or uptake. However, as Figure 4B reveals, after cell exposure to 729-SS-nlsEGFP for 24 h under standard culture conditions, followed by another 24 h incubation in fresh media, the cells showed green fluorescence of nlsEGFP distributed throughout the cytosol and nucleus, whereas no nlsEGFP was observable in the 737-SS-nlsEGFP treated cells, indicating that the proteins had been degraded by lysosomal proteases because of endolysosomal entrapment.

Flow cytometry results (Figure 4C) demonstrate a nine times higher mean fluorescence intensity for 729-SS-nlsEGFP treated cells compared with 737-SS-nlsEGFP treated cells. Considering

the similar molecular structure and cell uptake ability of 729-SS-nlsEGFP and 737-SS-nlsEGFP, we concluded that the different protein delivery efficiency may result from the distinct endosomal escape efficacy based on the oleic acid modification. An analogous comparison of the RNase A delivery efficiency of 729-SS-RNase A and 737-SS-RNase A gave consistent results (Figure 4D). KB cells treated with 729-SS-RNase A experienced significantly higher cytotoxicity compared with cells treated with 737-SS-RNase A. To further verify this conclusion, an erythrocyte leakage assay was performed to compare the lytic effects of 729-SS-nlsEGFP and 737-SS-nlsEGFP (Figure 4E) or 729-SS-RNase A and 737-SS-RNase A (Figure 4F) on lipid membranes. A potent lytic activity was observed for 729-SS-nlsEGFP both at physiological pH and early endosomal pH, whereas, in sharp contrast, 737-SS-nlsEGFP displayed no significant hemolysis under these conditions (Figure 4E). Similar findings were made in hemolysis studies of the RNase A conjugates; again, 729-SS-RNase A caused far more erythrocyte lysis than 737-SS-RNase A (Figure 4F). These results are well consistent with the cell metabolic activity assays (Figure 4D) after RNase A transductions. Also the oleic acid modified nontargeted oligomer 728 presented higher nlsEGFP and RNase A delivery efficiency than the control oligomer 937 (Figure S8, Supporting Information). The erythrocyte leakage assay of plain oligomers (without protein conjugation, Figure S9, Supporting Information) also showed a higher lytic activity of the oleic acid modified oligomers (728, 729) than the oligomers without oleic acid (937, 737). A direct effect of the oligomers on cell viability however could be excluded (Figure S10, Supporting Information). Furthermore, analogous oligomer conjugates of the nontoxic nlsEGFP protein did not mediate cytotoxicity (more than 80% metabolic activity of treated cells; Figure S11, Supporting Information).

3. Conclusions

Solid-phase assisted chemical synthesis presents an opportunity for novel chemical evolution of sequence-defined macromolecules for their use as drug and nucleic acid carriers.[23] Based on our former work, establishing a library of more than 900 precise sequence-defined oligoaminoamide oligomers,[13a,15,16] we further expand their application for targeted intracellular protein transduction and cancer therapy. Screening a small library of selected candidates, we identified sequence defined oligomers comprising PEG as hydrophilic shielding agent and optionally folic acid as targeting ligand as potent intracellular transduction agents for proteins covalently conjugated via bioreversible disulfide bonds. All evaluated oligomers present encouraging cellular association and internalization of protein as evidenced by nlsEGFP delivery. However, only the two-arm oligomers which were terminally modified with oleic acids showed both efficient cytosolic and nuclear delivery, and intracellular persistence of nlsEGFP. The oleic acid modification was a molecular requirement in conjugates for nanoparticle formation with medium small size of 25–35 nm, for destabilizing target lipid membranes enhancing cytosolic delivery, and altogether for efficient protein transduction. Folate-containing receptor targeted oligomer conjugates presented superior nlsEGFP transfection efficiency over the nontargeted control oligomer conjugates. Furthermore, choosing RNase A as a cargo protein for cancer therapy, the oleic acid modified two-arm oligomers again showed the most significant antitumoral effect. These results demonstrate the oleic acid modified sequence defined oligoaminoamide oligomers as a novel and promising nanocarrier for targeted intracellular protein delivery and cancer therapy.

4. Experimental Section

Materials: RNase A from bovine pancreas, FITC, SPDP, L-glutathione reduced (GSH), ethylenediaminetetraacetic acid (EDTA), DL-dithiothreitol (DTT) were purchased from Sigma-Aldrich, HEPES from Biomol GmbH. BCA protein assay reagents were purchased from Thermo Scientific. Antibiotics, fetal calf serum (FCS) and cell culture media were bought from Life Technologies or Sigma-Aldrich. Recombinant nlsEGFP was produced as previously reported.[20]

Cell Culture: Human KB cells were grown in folic acid free RPMI-1640 medium, supplemented with 10% FCS, 100 U mL^{-1} penicillin, 100 µg mL^{-1} streptomycin, and 4×10^{-3} M stable glutamine. Neuro-2a cells were grown in Dulbecco's modified Eagle's medium (DMEM), supplemented with 1 g L^{-1} glucose, 10% FCS, 100 U mL^{-1} penicillin, 100 µg mL^{-1} streptomycin, and 4×10^{-3} M stable glutamine. MCF-7 cells were grown in DMEM, supplemented with 4.5 g L^{-1} glucose, 20% FCS, 1×10^{-3} M sodium pyruvate, 100 U mL^{-1} penicillin, 100 µg mL^{-1} streptomycin, and 4×10^{-3} M stable glutamine. All cells were cultured at 37 °C in an incubator with 5% CO_2 and humidified atmosphere.

Fluorescein-Modified RNase A: RNase A (6 mg, 0.438 µmol) was dissolved in sodium carbonate-bicarbonate buffer (2 mL, 0.1 M, pH 9.0). Then FITC (1.314 µmol) was dissolved in DMSO (5 mg mL^{-1}) and added to the RNase A solution. After a 2 h incubation at 25 °C, the FITC modified RNase A was purified by size-exclusion chromatography via a Sephadex G25 superfine column using PBS buffer (1×10^{-3} M EDTA, pH 7.4) as the mobile phase. The purified RNase A-FITC was concentrated by Amicon Ultra centrifugal filter units (Millipore; MWCO 3000 Da). Protein concentration was measured by BCA assay as instructions. The whole experiment process was protected from light.

Protein Modification with SPDP: Modification of nlsEGFP. nlsEGFP (6 mg, 0.19 µmol) was dissolved in PBS buffer (2 mL, pH 7.4) containing 1×10^{-3} M EDTA. Then SPDP (1.14 µmol) was dissolved in DMSO (50 µL) and added to the nlsEGFP solution. After a 2 h incubation at 37 °C, the resulting SPDP modified nlsEGFP was purified by size-exclusion chromatography on a Sephadex G25 superfine column using HEPES buffer (pH 8.5, 0.3 M) as the mobile phase. Protein concentration was measured by BCA assay as instructions. The molar ratio of SPDP to nlsEGFP could be quantified by calculating the change in absorbance at 343 nm after reducing samples of the SPDP modified nlsEGFP with DTT using an extinction coefficient of 8080 M^{-1} cm^{-1}.

Modification of RNase A or RNase A-FITC: RNase A (6 mg, 0.438 µmol) or RNase A-FITC (6 mg) was dissolved in PBS buffer (2 mL, pH 7.4) containing 1×10^{-3} M EDTA. Then SPDP (2.19 µmol) was dissolved in DMSO (100 µL) and added to the RNase A solution or RNase A-FITC solution. After a 2 h incubation at 37 °C, the resulting SPDP modified proteins were purified respectively by size-exclusion chromatography on a Sephadex G25 superfine column using HEPES buffer (pH 8.6, 0.1 M) as the mobile phase. Protein concentration was measured by BCA assay as instructions. The molar ratio of SPDP to RNase A or RNase A-FITC could be quantified by calculating the change in absorbance at 343 nm after reducing samples of the SPDP modified RNase A with DTT using an extinction coefficient of 8080 M^{-1} cm^{-1}.

Conjugation of Proteins with Oligomers: Oligoaminoamides of the oligomer library were synthesized by solid phase-assisted synthesis using the properly fmoc, tboc-protected artificial oligoamino acids (Stp and Sph)[24] as reported before.[13a,14a,15,18d,24] The SPDP modified nlsEGFP was divided into 0.25 mg per aliquot and dissolved in HEPES

buffer (0.5 mL, pH 8.5, 0.3 M). For SPDP modified RNase A or RNase A-FITC, the proteins were divided into 0.25 mg per aliquot and dissolved in HEPES buffer (0.25 mL, pH 8.6, 0.1 M). Various oligomers dissolved in water (50 mg mL^{-1}; for 728 and 729, 25 mg mL^{-1}) were added to the above modified protein solutions, respectively, as twice the molar quantity of covalently attached SPDP. This ratio was empirically found as optimum oligomer/cargo ratio. After a 15 min incubation at 20 °C, the formed conjugates were shock-frozen in liquid nitrogen and stored at –80 °C or used for further experiments immediately.

Cellular Association: KB cells were seeded into 24-well plates at a density of 50 000 cells per well. After 24 h, the 500 µL medium was replaced with fresh serum-containing medium. Then, the various nlsEGFP conjugates (final concentration 1×10^{-6} M) or 729-SS-RNase A-FITC conjugate (final concentration 2×10^{-6} M) were added into each well and incubated on ice for 45 min. Then, the cells were washed with 500 µL PBS, detached with trypsin/EDTA and diluted with PBS containing 10% FCS. After centrifugation, the cells were taken up in 600 µL PBS containing 10% FCS. The cellular fluorescence was assayed by excitation of nlsEGFP or FITC at 488 nm and detection of emission at 510 nm with a Cyan ADP flow cytometer (Dako, Hamburg, Germany). Cells were appropriately gated by forward/sideward scatter and pulse width for exclusion of doublets, and counterstained with DAPI (4′,6-diamidino-2-phenylindole) to discriminate between viable and dead cells. Minimum ten thousand gated cells per sample were collected. Data were recorded with Summit software (Summit, Jamesville, NY). Analysis was done by FlowJo 7.6.5 flow cytometric analysis software. All experiments were performed in triplicates.

Cellular Internalization: KB cells were seeded into 24-well plates at a density of 50 000 cells per well. After 24 h, the 500 µL medium was replaced with fresh serum-containing medium. Then, the various nlsEGFP conjugates (final concentration 1×10^{-6} M) or 729-SS-RNase A-FITC conjugate (final concentration 2×10^{-6} M) was added into each well and incubated at 37 °C for 45 min or incubated at 37 °C for 24 h, followed by an incubation of 24 h in fresh media. Then, the cells were washed with 500 µL PBS, detached with trypsin/EDTA, and diluted with PBS containing 10% FCS. After centrifugation, the cells were taken up in 600 µL PBS (pH 4.0) to extinguish the outside fluorescence. The cellular fluorescence was assayed by excitation of nlsEGFP or FITC at 488 nm and detection of emission at 510 nm with a Cyan ADP flow cytometer (Dako, Hamburg, Germany). Cells were appropriately gated by forward/sideward scatter and pulse width for exclusion of doublets, and counterstained with DAPI (4′,6-diamidino-2-phenylindole) to discriminate between viable and dead cells. Minimum 10 000 gated cells per sample were collected. Data were recorded with Summit software (Summit, Jamesville, NY). Analysis was done by FlowJo 7.6.5 flow cytometric analysis software. All experiments were performed in triplicates.

Particle Size and Zeta Potential: Particle size and zeta potential of protein conjugates were measured by dynamic laser-light scattering using a Zetasizer Nano ZS (Malvern Instruments, Worcestershire, UK). For particle size measurement, protein conjugates were measured in 100 µL HEPES buffer (pH 7.4, 20×10^{-3} M) at a concentration of 0.25 mg mL^{-1}. Then the protein conjugate solution was diluted to 800 µL for zeta potential measurement.

Erythrocyte Leakage Assay: Preserved human red blood cells (obtained from LMU Clinics—Campus Grosshadern, Munich, Germany) were washed with PBS for several times. After centrifugation, the erythrocyte pellet was diluted to 5×10^7 erythrocytes per mL with PBS (buffered to the indicated pH). The protein conjugates or plain oligomers were diluted to 75 µL with above PBS, respectively, and added to a V-bottom 96-well plate (NUNC, Denmark). Control wells had buffer with 1% Triton X-100 for 100% lysis. Then, 75 µL erythrocyte suspension was added to each well, resulting in a final concentration of 1×10^{-6} M nlsEGFP conjugates or 2×10^{-6} M RNase A conjugates or 5×10^{-6} M plain oligomers per well. The plates were incubated under constant shaking for 1 h at 37 °C. After centrifugation, 80 µL supernatant was analyzed for hemoglobin release at 405 nm with a microplate reader (Tecan Spectrafluor Plus, Tecan, Switzerland). PBS with different indicated pH was used as negative control. Relative hemolysis was defined as hemolysis (%) = (A_{405} (conjugate treated) – A_{405} (PBS treated))/(A_{405} (Triton X treated) – (A_{405} (PBS treated)) × 100.

Fluorescence Microscopy: KB cells were seeded into 8 well Nunc chamber slides (Thermo Scientific, Germany) coated with collagen at a density of 10 000 cells per well. After 24 h, the 300 µL medium was replaced with fresh medium. Subsequently, the various nlsEGFP conjugates were added into each well (final concentration 1×10^{-6} M) and incubated at 37 °C for 24 h, followed by a 24 h incubation in fresh media. Then, the live cells were observed on a Zeiss Axiovert 200 fluorescence microscope (Jena, Germany). For 729-SS-RNase A-FITC transfection, the same experiment was performed, but the final concentration was 2×10^{-6} M and incubation was at 37 °C for 45 min. Then, the cells were washed with 300 µL PBS and fixed with 4% paraformaldehyde, followed by nuclei staining with DAPI (1 µg mL^{-1}). A 63× magnification DIC oil immersion objective (Plan-APOCHROMAT) and appropriate filter sets for analysis of EGFP or DAPI were used. Data were analyzed and processed by AxioVision Rel. 4.8 software (Zeiss, Jena, Germany).

RNase A Transfection: For the screening experiment of various RNase A conjugates, KB cells were seeded into 96-well plates at a density of 10 000 cells per well. After 24 h, the medium was replaced with 80 µL fresh medium. Subsequently, the various RNase A conjugates (final concentration 4×10^{-6} M), RNase A-PDP (final concentration 4×10^{-6} M), polymers (final concentration 16×10^{-6} M), and mixtures of free RNase A (final concentration 4×10^{-6} M) and polymers (final concentration 16×10^{-6} M) were diluted to 20 µL with PBS, respectively, added to each well and incubated at 37 °C for 4 h, followed by a 44 h incubation in fresh media. Afterward, MTT solution (10 µL per well, 5.0 mg mL^{-1}) was added. After incubation for 2 h, the medium was removed and the 96-well plates were stored at –80 °C for at least 1 h. 100 µL DMSO per well were added to dissolve the purple formazan product. The optical absorbance was measured at 590 nm, with a reference wavelength of 630 nm, by a microplate reader (Tecan Spectrafluor Plus, Tecan, Switzerland). The relative cell viability (%) related to control wells treated only with 20 µL PBS was calculated as ([A] test/[A] control) × 100%. All experiments were performed in triplicates.

For investigation of protein concentration-dependent cytotoxicity of RNase A conjugates on folate-receptor-positive or negative cells and the structure–activity relationship, KB cells, MCF-7 cells, or Neuro-2a cells were seeded into 96-well plates at a density of 10 000 cells per well. After 24 h, the medium was replaced with 80 µL fresh medium. Subsequently, the RNase A conjugates (final concentration 0.25; 0.5; 1.0; 2.0; 4.0×10^{-6} M), RNase A-PDP (final concentration 0.25; 0.5; 1.0; 2.0; 4.0×10^{-6} M), oligomers (final concentration 1.0; 2.0; 4.0; 8.0; 16.0×10^{-6} M) were diluted to 20 µL with PBS, respectively, added to each well and incubated at 37 °C for 4 h, followed by a 44 h incubation in fresh media. Afterward, cell viability was measured by the MTT assay as describe above.

Cell Viability Assay of nlsEGFP Conjugates: KB cells were seeded into collagen coated 96-well plates at a density of 10 000 cells per well. After 24 h, the medium was replaced with 80 µL fresh medium. Subsequently, the nlsEGFP conjugates (final concentration 0.1; 0.25; 0.5; 1.0; 1.5×10^{-6} M) and nlsEGFP-PDP (final concentration 0.1; 0.25; 0.5; 1.0; 1.5×10^{-6} M) were diluted into 20 µL with PBS, respectively, added into each well, and incubated with cells at 37 °C for 24 h, then the medium was replaced with 100 µL fresh medium, followed by another 24 h incubation. Afterward, cell viability was measured by the MTT assay as describe above.

Statistical Analysis: The statistical significance of experiments were analyzed using the Tukey test, $p < 0.05$ was considered statistically significant in all analyses (95% confidence interval).

Supporting Information

Supporting Information is available from the Wiley Online Library or from the author.

Acknowledgements

Peng Zhang, Dongsheng He, and Xiaowen Liu appreciate receiving China Scholarship Council fellowships as support to their PhD studies at Ludwig-Maximilians-University, Munich, Germany. The authors also acknowledge the financial support from the DFG Excellence Cluster Nanosystems Initiative Munich (NIM).

Received: July 29, 2015
Revised: September 3, 2015
Published online: September 23, 2015

[1] a) B. Leader, Q. J. Baca, D. E. Golan, *Nat. Rev. Drug Discovery* **2008**, *7*, 21; b) G. Walsh, *Nat. Biotechnol.* **2014**, *32*, 992.
[2] a) L. H. Pai, R. Wittes, A. Setser, M. C. Willingham, I. Pastan, *Nat. Med.* **1996**, *2*, 350; b) R. J. Kreitman, M. Stetler-Stevenson, I. Margulies, P. Noel, D. J. Fitzgerald, W. H. Wilson, I. Pastan, *J. Clin. Oncol.* **2009**, *27*, 2983.
[3] T. Schirrmann, J. Krauss, M. A. Arndt, S. M. Rybak, S. Dubel, *Expert Opin. Biol. Ther.* **2009**, *9*, 79.
[4] M. Qiao, L. D. Zu, X. H. He, R. L. Shen, Q. C. Wang, M. F. Liu, *Cell Res.* **2012**, *22*, 1199.
[5] a) P. A. Leland, R. T. Raines, *Chem. Biol.* **2001**, *8*, 405; b) V. A. Shlyakhovenko, *Exp. Oncol.* **2009**, *31*, 127.
[6] Z. Gu, A. Biswas, M. Zhao, Y. Tang, *Chem. Soc. Rev.* **2011**, *40*, 3638.
[7] N. Murthy, Y. X. Thng, S. Schuck, M. C. Xu, J. M. Frechet, *J. Am. Chem. Soc.* **2002**, *124*, 12398.
[8] M. Ray, R. Tang, Z. Jiang, V. M. Rotello, *Bioconjug. Chem.* **2015**, *26*, 1004.
[9] Y. Lee, T. Ishii, H. J. Kim, N. Nishiyama, Y. Hayakawa, K. Itaka, K. Kataoka, *Angew. Chem. Int. Ed. Engl.* **2010**, *49*, 2552.
[10] M. Wang, K. Alberti, S. Sun, C. L. Arellano, Q. Xu, *Angew. Chem.* **2014**, *126*, 2937.
[11] S. J. Kaczmarczyk, K. Sitaraman, H. A. Young, S. H. Hughes, D. K. Chatterjee, *Proc. Natl. Acad. Sci. USA* **2011**, *108*, 16998.
[12] a) R. K. June, K. Gogoi, A. Eguchi, X. S. Cui, S. F. Dowdy, *J. Am. Chem. Soc.* **2010**, *132*, 10680; b) N. Nischan, H. D. Herce, F. Natale, N. Bohlke, N. Budisa, M. C. Cardoso, C. P. Hackenberger, *Angew. Chem. Int. Ed. Engl.* **2015**, *54*, 1950.
[13] a) D. Schaffert, C. Troiber, E. E. Salcher, T. Frohlich, I. Martin, N. Badgujar, C. Dohmen, D. Edinger, R. Klager, G. Maiwald, K. Farkasova, S. Seeber, K. Jahn-Hofmann, P. Hadwiger, E. Wagner, *Angew. Chem. Int. Ed. Engl.* **2011**, *50*, 8986; b) U. Lächelt, E. Wagner, *Chem. Rev.* **2015**, DOI:10.1021/cr5006793.
[14] a) U. Lächelt, P. Kos, F. M. Mickler, A. Herrmann, E. E. Salcher, W. Rödl, N. Badgujar, C. Bräuchle, E. Wagner, *Nanomed.: NBM* **2014**, *10*, 35; b) P. Kos, U. Lächelt, A. Herrmann, F. M. Mickler, M. Doblinger, D. He, A. Krhac Levacic, S. Morys, C. Brauchle, E. Wagner, *Nanoscale* **2015**, *7*, 5350.
[15] T. Fröhlich, D. Edinger, R. Klager, C. Troiber, E. Salcher, N. Badgujar, I. Martin, D. Schaffert, A. Cengizeroglu, P. Hadwiger, H. P. Vornlocher, E. Wagner, *J. Controlled Release* **2012**, *160*, 532.
[16] U. Lächelt, V. Wittmann, K. Muller, D. Edinger, P. Kos, M. Hohn, E. Wagner, *Mol. Pharmaceutics* **2014**, *11*, 2631.
[17] K. Maier, I. Martin, E. Wagner, *Mol. Pharmaceutics* **2012**, *9*, 3560.
[18] a) E. P. Feener, W. C. Shen, H. J. Ryser, *J. Biol. Chem.* **1990**, *265*, 18780; b) G. Saito, J. A. Swanson, K. D. Lee, *Adv. Drug Delivery Rev.* **2003**, *55*, 199; c) B. A. Kellogg, L. Garrett, Y. Kovtun, K. C. Lai, B. Leece, M. Miller, G. Payne, R. Steeves, K. R. Whiteman, W. Widdison, H. Xie, R. Singh, R. V. Chari, J. M. Lambert, R. J. Lutz, *Bioconjug. Chem.* **2011**, *22*, 717; d) P. M. Klein, K. Müller, C. Gutmann, P. Kos, A. Krhac Levacic, D. Edinger, M. Hohn, J. C. Leroux, M. A. Gauthier, E. Wagner, *J. Controlled Release* **2015**, *205*, 109; e) P. M. Klein, E. Wagner, *Antioxid. Redox Signaling* **2014**, *21*, 804.
[19] C. Troiber, D. Edinger, P. Kos, L. Schreiner, R. Kläger, A. Herrmann, E. Wagner, *Biomaterials* **2013**, *34*, 1624.
[20] K. Maier, E. Wagner, *J. Am. Chem. Soc.* **2012**, *134*, 10169.
[21] A. Erazo-Oliveras, K. Najjar, L. Dayani, T. Y. Wang, G. A. Johnson, J. P. Pellois, *Nat. Methods* **2014**, *11*, 861.
[22] a) C. Dohmen, T. Fröhlich, U. Lachelt, I. Rohl, H.-P. Vornlocher, P. Hadwiger, E. Wagner, *Mol. Ther. Nucleic Acids* **2012**, *1*, e7; b) C. Dohmen, D. Edinger, T. Fröhlich, L. Schreiner, U. Lächelt, C. Troiber, J. Rädler, P. Hadwiger, H. P. Vornlocher, E. Wagner, *ACS Nano* **2012**, *6*, 5198.
[23] a) X. L. Wang, R. Jensen, Z. R. Lu, *J. Controlled Release* **2007**, *120*, 250; b) L. Hartmann, H. G. Börner, *Adv. Mat.* **2009**, *21*, 3425.
[24] a) D. Schaffert, N. Badgujar, E. Wagner, *Org. Lett.* **2011**, *13*, 1586; b) E. E. Salcher, P. Kos, T. Fröhlich, N. Badgujar, M. Scheible, E. Wagner, *J. Controlled Release* **2012**, *164*, 380.